# Biocompatible/Bioabsorbable Silver Nanocomposite Coatings

**Ammar T. Qureshi,[1] W. Todd Monroe,[1] Mandi J. Lopez,[2] Marlene E. Janes,[3] Vinod Dasa,[4] Sunggook Park,[5] Alborz Amirsadeghi,[5] Daniel J. Hayes[1]**

[1]*Department of Biological and Agricultural Engineering, Louisiana State University and Agricultural Center, Baton Rouge, Louisiana 70803*
[2]*Department of Veterinary Clinical Sciences, Louisiana State University, Baton Rouge, Louisiana 70803*
[3]*Department of Food Science, Louisiana State University Agricultural Center, Baton Rouge, Louisiana 70803*
[4]*Department of Orthopedics, Louisiana State University Health Science Center, New Orleans, Louisiana 70115*
[5]*Department of Mechanical Engineering, Louisiana State University, Baton Rouge, Louisiana 70803*

Received 11 June 2010; accepted 28 September 2010
DOI 10.1002/app.33481
Published online 12 January 2011 in Wiley Online Library (wileyonlinelibrary.com).

**ABSTRACT:** A novel biomass-mediated method to synthesize cellulose-stabilized silver nanoparticles (SNPs) and incorporate them into biocompatible/bioabsorbable poly-L-lactic acid (PLLA) for producing SNP–PLLA nanocomposite thin films was developed and the antimicrobial efficacy and biocompatibility of the SNP–PLLA films were studied. The formation and coating morphology of SNPs were characterized with UV–visible spectrophotometry and transmission electron microscopy (TEM), and the release rate of silver ion from the SNP–PLLA films was determined by inductively coupled plasma-optical emission spectrometry. Antimicrobial testing of the SNP–PLLA films performed with *Staphylococcus aureus* and *Escherichia coli* according to ISO 22196 standards demonstrated that the SNP–PLLA nanocomposite films with a SNP concentration of 700 ppm reduced colonies forming unit (CFU) counts by 99.8 and 99.99%, respectively. Despite the significant antimicrobial activity, the nanocomposite films with the same SNP concentration had little effect on the viability of human HeLa cells. This strategy that has been developed for the synthesis of nanoparticles and the formation of composite films demonstrates promise for reducing perioperative surgical site infections associated with indwelling devices. © 2011 Wiley Periodicals, Inc. J Appl Polym Sci 120: 3042–3053, 2011

**Key words:** silver nanoparticles (SNP); biocompatible/bioabsorbable thin film coatings; PLLA; hydroxypropyl cellulose; indwelling medical implants; biofilm reduction; nanoparticle cytotoxicity

## INTRODUCTION

The implantation of indwelling devices is often complicated by infections with biofilm-forming microbes that are resistant to a number of antimicrobial agents.[1,2] Biofilms are glue-like substances composed of a matrix of excreted polymeric compounds called exopolysaccharides (EPS) that are formed by bacteria.[3] The biofilm allows bacteria to adhere to medical implants composed of metallic, polymeric, ceramic, and composite substances and potentially protects bacterial colonies from antimicrobial therapies. A variety of active and passive strategies including the use of antibiotics, inorganic salts,[4,5] inorganic nanomaterials,[6,7] and organic compounds[8,9] have been employed to impart antimicrobial properties to materials used for indwelling devices. These strategies have produced satisfactory results for acute indwelling devices like wound dressings,[10] central venous catheters,[11] and endotracheal tubes[12–14] but not in chronic devices.

Silver, in a variety of forms, is among the device-based antimicrobial solutions that are currently commercially available, and it has a successful history of safe and efficacious use against a broad spectrum of gram-positive and gram-negative microbial agents.[15–17] Exposure to relatively low concentrations of oligodynamic antimicrobial compounds like silver can result in substantial reduction of viable microbial organisms. While the ionic form of silver, $Ag^+$, is considered the primary active agent,[18] recent research indicates that the nanoscale metal form of the compound may have some unique antimicrobial attributes.[19] Various silver compounds have been used as antimicrobial agents in many healthcare-related applications including pathogen control, prophylaxis, and treatments. Salts,[20–23] zeolites,[24–26] and thin film metal coatings[27] have some utility as silver ion sources for medical devices, but concerns regarding cost, performance, bioavailability, chemical stability, and safety have limited the broader adoption of these delivery vehicles in indwelling device applications. Silver nanoparticles

*Correspondence to:* D. J. Hayes (danielhayes@lsu.edu).
Contract grant sponsors: LSU AgCenter.

(SNPs) provide a thermal, chemical, and photostable reservoir of metal atoms that are uniquely suited to polymer composite formation while remaining available for conversion to the active ionic compound upon exposure to physiological solutions. Several silver containing nanocomposites have been described for use in anti-infective coatings; silver bromide in pyridinium polymer,[21] silver bromide in amphiphilic graft copolymer,[28] silver nanoparticles in carboxymethylchitin,[29] photoreduced silver in polyvinyl alcohol,[30] and sputtered silver in plasma deposited polymer.[31]

Several biomass mediated and biological approaches have been explored for SNP synthesis[32–43] but to date, none of these efforts have resulted in a high-purity and high-yield synthesis that produces a chemically stable product compatible with bioabsorbable/biocompatible thin film coatings. This manuscript contains a description of a hydroxypropyl cellulose-mediated SNP synthesis and purification method yielding high-purity, biocompatible, nanomaterial powders and colloidal solutions with tunable chemical properties. Additionally, the applicability of this silver nanomaterial-based antimicrobial compound as a chemo-prophylactic agent in bioabsorbable/biocompatible poly-L-lactic acid (PLLA) thin film coatings is evaluated. Concentrations and contact times required for *in vitro* elimination of known titers of two model organisms, *Staphylococcus aureus* and *Escherichia coli* is determined as well as coating adhesion strength.

While the cosmetic condition argyria is the only known acute systemic toxicity associated with chronic silver exposure, silver has been demonstrated to induce cytotoxicity *in vitro* and thus toxicity remains a concern for silver containing devices.[44] We quantitatively measure the cytotoxicity of SNP containing PLLA films against HeLa cells by flow cytometry and qualitatively evaluate cell health by optical microscopy to determine a SNP concentration range that is efficacious in reducing viable bacteria but has minimal human cell cytotoxicity. Silver release rate and nanoparticle erosion as a function of particle concentration and thin film composition is characterized, along with bioabsorbable film response to exposure to simulated physiological solution.

## MATERIALS AND METHODS

### Materials

Silver nitrate $> 99\%$, hydroxypropyl cellulose (HPC) with an average molecular weight of 80 kDa, sodium hydroxide (NaOH) at 98%, formaldehyde 36.5–38%, antifoam A concentrate, PLLA with average molecular weight of 100–150 kDa, 2-butanone HPLC grade $\geq 99.7\%$, brain heart infusion agar (BHI), nutrient agar, and technical agar were purchased from Sigma Aldrich (Sigma Chemical Co, St Louis, MO). Dulbecco's Modified Eagle's Medium-reduced serum (DMEM-RS), Dulbecco's Phosphate-Buffered Saline (DPBS), and 0.25% Trypsin were purchased from HyClone Laboratories (Logan, UT). SYTOX Green was purchased from Invitrogen (Carlsbad, CA). 3-Aminopropyltriethoxysilane (APTS) linker was purchased from Gelest (Morrisville, PA) and 3% hydrogen peroxide ($H_2O_2$) was purchased from Humco (Texarkana, TX). All solvents purchased were of analytical grade.

### Microbiology test organisms

*Escherichia coli* (ATCC 29522) and *Staphylococcus aureus* (ATCC 6538) were grown (BD Falcon, Franklin Lakes, NJ) in Nutrient Agar and BHI broth, respectively, and incubated at 37°C.

### Cell culture

HeLa cells (American Type Culture Collection) were maintained in 25-$cm^2$ flasks (BD Falcon, Franklin Lakes, NJ) with 5 mL of Dulbecco's Modified Eagle's Medium-reduced serum (DMEM-RS) supplemented with 3% Fetal Bovine Serum (FBS) and incubated at 37°C and 5% $CO_2$. For necrotic control,[45] HeLa cells were plated at a density of $2 \times 10^6$ cells/mL in 12-well tissue culture plates (Falcon, Franklin Lakes, NJ). For exposure to PLLA thin films, $2.6 \times 10^6$ cells/mL were plated with in clear $60 \times 15$-mm petri dishes (VWR International, LLC, West Chester, PA). Cells were allowed to adhere and grow for 24 h before every SNP treatment.

### Methods

#### Biomass-mediated SNP synthesis

Using a syringe pumps (KD Scientific 200, Holliston MA), 35 mL of each 125 m*M* $AgNO_3$ and 61.5 m*M* formaldehyde (HCOH) were added at 0.5 mL/min, to a predissolved solution containing 0.5 g NaOH, 0.31 g HPC, 330 mL deionized (DI) water, and 5 μL antifoaming agent, Antifoam A, at room temperature (RT). This resulted in the synthesis of 25–75 nm SNP. Purification was accomplished by thermal flocculation of the solution and removal of supernatant. The SNP solution was heated to 70–75°C under static conditions resulting in flocculation and precipitation. After precipitation, the supernatant was removed and the pellet was resuspended in water at RT. This process was repeated four times and the resulting pellet dried and ground yielding a $\sim 98\%$ pure SNP powder. Samples were taken when 10, 20, 30, and 35 mL of reactants had been added by syringe pumps to study the time evolution of SNP

over time by Genesys6 (Thermo Scientific, Madison WI) UV–Visible Spectrophotometer.

### Characterization of SNP

For TEM characterization, 5 μL of 800 ppm SNP solution was pipetted on Carbon/Copper 20–30 nm grids (EMS, Hatfield, PA), air dried, and evaluated with a JEOL 100CX.

### PLLA thin film coatings

A 1% PLLA polymer was dissolved in butanone solution by stirring for 0.5 h at 75–80°C. The butanone volume was maintained to keep the polymer stable while the solution was cooled to RT with continuous stirring until the solution clouded. Varying concentrations of colloidal SNP in 100 mL methanol were then added to 10 mL of PLLA polymer solution to create a dilution ladder. A total of 10 mL of SNP containing PLLA solution was poured into the treated dish and solvent was allowed to evaporate for 24 h at RT in a fume hood. After evaporation, the substrates with dried coatings were then extracted in DI water for 24 h with DI water exchanges every 12 h, followed by incubation at 50°C for 24 h to extract residual solvent. The coated substrates were sterilized by autoclaving at 117.2 kPa for 32 min before antimicrobial and cytotoxicity experiments.

Two PLLA coatings with SNP concentrations of 700 and 5000 ppm along with two controls, coatings with No SNP and No SNP with 100 μL of HPC, were characterized with a Stereoscan$^{TM}$ 260 scanning electron microscope (SEM) (Cambridge Scientific Instruments, Cambridge, UK) at 25 kV to study the thickness and surface characteristics of the coatings. Each sample was mounted on aluminum stubs with either Tubecote or colloidal graphite and sputter coated with a gold–palladium film in an Edwards *S*-150 sputter coater (Edwards High Vacuum Co. International, Wilmington, MA) to image the surface morphology in SEM.

The surface roughness of PLLA films containing varying amounts of SNP was measured using a commercial AFM system (Agilent 5500) in tapping mode. A conical silicon tip with a nominal tip radius 10–20 nm on aluminum back-coated cantilevers with a nominal spring constant of 7.4*N*/m (Budget Sensors, model All-in-one-Al; cantilever C) was used. The scanning was performed at a scanning rate of 0.2 Hz (1 μm/s) along the fast scan axis and a scan size of 5 × 5 μm$^2$. The fast scan axis was perpendicular to the longitudinal direction of the cantilever. The measurements were done at room temperature and a relative humidity of ~ 50%. The obtained topographic images were flattened but no further processing was performed. Roughness values were then obtained with image processing software; Gwyddion. Mean squared roughness (RMS) over 11 lines on each scanned area was measured and averaged.

### Antimicrobial activity

Quantitative antimicrobial testing with *Staphylococcus aureus* and *Escherichia coli* were conducted according to the ISO 22196 test methods with a detection limit of 30–300 bacterial colonies. Briefly, 300 μL of the inoculated bacterial cultures were exposed to either double- or triple-coated films for every SNP concentration for 24 h. A coating without SNP was also included in the dilution ladder as a control for each test organism to measure the efficacy of the coatings. The percentage reduction and colony forming unit (CFU) values were statistically analyzed using ANOVA.

The antimicrobial activity ($R$) was calculated using the following equation:

$$R = (U_t - U_0) - (A_t - U_0) = U_t - A_t$$

where $R$ is the antibacterial activity;

$U_0$ is the average of the common logarithm of the number of viable bacteria, in cells/cm$^2$, recovered from the untreated test specimens immediately after inoculation;

$U_t$ is the average of the common logarithm of the number of viable bacteria, in cells/cm$^2$, recovered from the untreated test specimens after 24 h;

$A_t$ is the average of the common logarithm of the number of viable bacteria, in cells/cm$^2$, recovered from the treated test specimens after 24 h.

### Silver release from PLLA coating

Coatings, prepared as above on 60 mm glass petri dishes, containing 700 ppm of SNP were exposed to 7 mL of PBS solution each for 7 days ($n = 2$). Daily, 1 mL PBS solution was collected from each sample, without replacing it with fresh PBS, at RT for ICP-OES analysis. Before injection, the solutions were incubated with 1 mL nitric acid, transferred to weighed ICP vials, agitated for 2.5 h, and diluted to a final volume of 10 mL with acidified water. The final vials are weighed and the diluted samples were run on Varian Vista MPX (Palo Alto, CA). A no-SNP containing control sample was also compared. Only the 700 ppm coating was tested for silver release due to superior antimicrobial and cytotoxicity results discussed in sections "Antimicrobial activity" and "Cytotoxicity of nanocomposite coatings." The 5000 ppm sample was not included in the experimental design due to its cytotoxic nature discussed in section "Cytotoxicity of nanocomposite coatings."

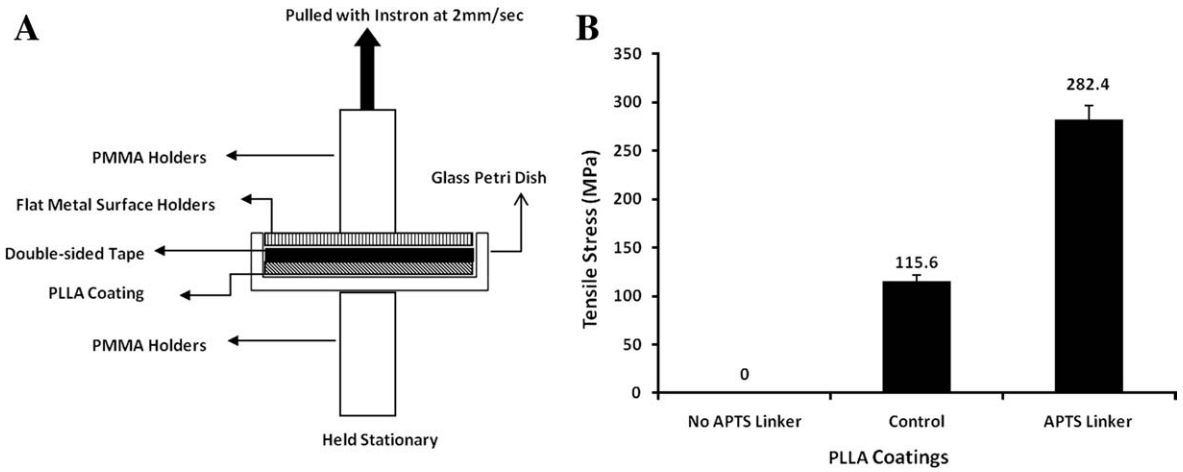


**Figure 1** A: Schematic for tensile adhesion testing of PLLA coatings on the glass surface. B: Tensile adhesion strength of PLLA coating with and without the APTS linker ($n = 2$).

### Cytotoxicity experiments on PLLA films

A 1 mL cell solution ($2 \times 10^6$ cell/mL) was plated on circular PLLA thin film coatings, 60 mm in diameter, containing varying concentration of SNP (700–5000 ppm) and incubated for 24 h at 37°C with 5% $CO_2$. For a necrotic control, HeLa cells were incubated for 18 h in fresh medium with 2 m*M* hydrogen peroxide ($H_2O_2$). After treatment, adhered HeLa cells were harvested by trypsinization (0.25% Trypsin), washed with 1 mL DPBS, pooled together with the detached HeLa cells, and centrifuged at 1800 rpm to obtain cell pellet. Cells were resuspended in 1 mL DPBS and stained with 5 μL of 500 μ*M* Sytox Green for 15 min in the dark, then centrifuged and fixed in 250 μL of 1% paraformaldehyde (PFA) solution in PBS for flow cytometric analysis of viability with a BD FACSCalibur cytometer (Franklin Lakes, NJ). For each sample, scatter and fluorescent data was collected for 30,000 cell events using Cellquest pro (BD Biosciences, San Jose, CA) and former analyzed using WinMDI 2.8 software (by Dr. J. Trotter, Scripps Institute, La Jolla, CA).

To study the morphology of the HeLa cell on PLLA films, 22 × 22 mm glass cover slips (Corning, NY) were coated with 1% PLLA (control) and PLLA–SNP, containing 700 and 5000 ppm silver, thin films and inserted into 12-well Tissue Cultured plates (BD Falcon, Franklin Lakes, NJ). A 1 mL cell solution, of cell density $2 \times 10^6$ cell/mL, was plated coated cover slips and cultured for 24 h at 37°C with 5% $CO_2$. The 12-well plates containing the PLLA-coated cover slips were imaged using Nikon FL microscope.

### Tensile testing

Two circular $SiO_x$ substrates, 60 × 15-mm, were coated with 2% γ-aminopropyltriethoxysilane (APTS) coupling agent for 4–5 min after which excess solution was removed. The substrate was then cured at 100°C for 2–3 min to improve adhesion before coating with PLLA. To test the tensile strength of the substrate, double-sided 3*M*™ 4026 tape (St. Paul, MN) was applied to the coatings cast on the glass surfaces and pulled in an orthogonal direction to the film surface with an Instron™ 8841 (Norwood, MA) mechanical testing machine at a speed of 2 mm/s to failure, whereas the holder with glass petri dish coated with PLLA nanocomposite was held immobile [Fig. 1(A)]. The test was conducted on PLLA coatings attached to the glass surface with and without the APTS linker to quantify the impact of the APTS linker on adhesion strength. A noncoated control sample was also analyzed for comparison.

## RESULTS

### Biomass-mediated SNP synthesis

A time-evolution study was performed during the synthesis process to examine the progression and behavior of synthesized SNP as reactants were added. Samples (1 mL) were collected from the final beaker after 10, 20, 30, and 35 mL of silver nitrate and formaldehyde had been added. The four samples clearly showed the progression of the synthesis reaction with a distinct color change from grayish–black at 20 min (10 mL sample) to dark gray at 70 min (35 mL sample). When the 35 mL sample was diluted with DI water, the solution had a golden-brown color, suggesting the presence of SNP. Two established techniques, UV–VIS spectrophotometry and TEM, were used to confirm the presence of polydispersed SNPs. The formation of silver particles was indicated by a silver surface plasmon resonance peak at 415 in UV–Vis spectra nm in all of the time-evolution samples [Fig. 2(A)]. The plasmon resonance

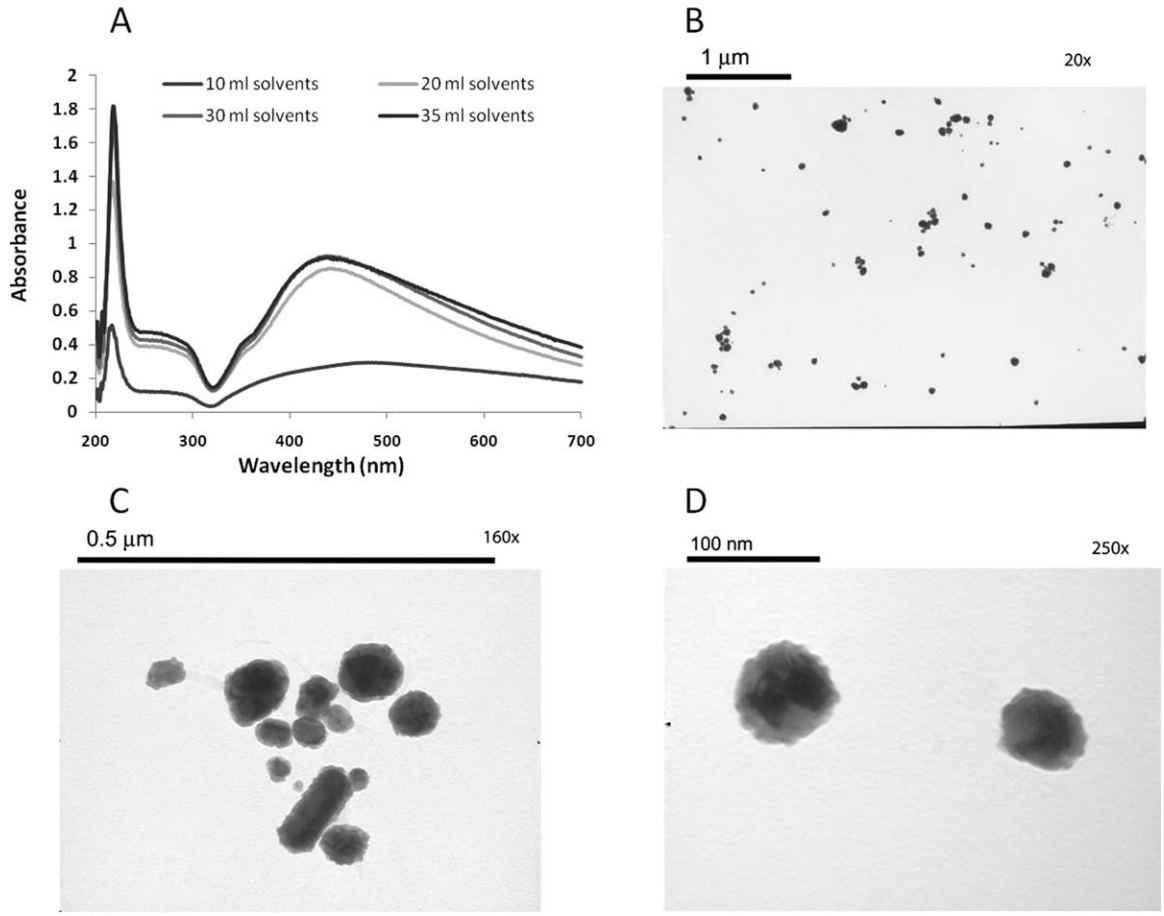


**Figure 2** A: UV–Vis Spectrum of SNP synthesis reaction indicating the time evolution of the synthesis process. TEM images of SNP with increasing magnification (B) ×20, (C) ×160, and (D) ×250.

peak was not red-shifted right upon the addition of reactants as may be expected with increases in the particle size, whereas the absorbance value increased from 0 to 2.0. This observation is likely related to an increase in SNP concentration versus an increase in particle size.[46] Analysis of the SNP morphology with TEM revealed a size distribution from 25 to 75 nm [Fig. 2(B,C)]. The lighter colored areas of the particles [Fig. 2(D)] are likely HPC-rich regions, whereas the darker areas are silver laden regions. The HPC molecule acts as the precursor substrate to attract silver nitrate through hydrogen bonding.[47] The SNP are then formed as hydroxyl groups are reduced by formaldehyde. The HPC substrate promotes even distribution of the SNP nucleation points, producing a dispersed and highly concentrated SNP solution.

## Characterization of PLLA film

A complete table of samples and associated characterization techniques can be found in Table I. The PLLA nanocomposite thin films were cast on glass petri dishes in an effort to optimize the thickness, substrate adhesion, and silver release. SEM images of PLLA nanocomposite demonstrated that the casting process yielded uniform thin films $\sim$ 50 μm thick [Fig. 3(D,F)] with a corresponding volume of 9.82 $mm^3$. The composite surface morphology was greatly influenced by the HPC content of the coatings. The bulky molecular structure of HPC introduces artifacts in the morphology of the composites resulting in a more amorphous structure. The surface of PLLA coating with HPC [Fig. 3(A)] appears smoother and more homogenous than that of PLLA coating without HPC [Fig. 3(B)]. Similarly, surfaces with 5000 ppm [Fig. 3(C)] films appear smoother and more homogenous than those containing 700 ppm SNP [Fig. 3(E)]. The particle to volume ratio for 700 and 5000 ppm coatings is estimated to be $3.98 \times 10^{16}$ and $2.84 \times 10^{17}$ SNP particles per cubic millimeter of the film, respectively, based on these SEM images.

The surface roughness analysis by AFM confirmed the results observed by SEM. The average root mean square roughness (RMS) of the non-SNP control, 700 ppm, and 5000 ppm films was 9.2 ± 0.2% nm, 7.2 ± 0.24% nm, and 4.7 ± 0.17% nm, respectively, and a clear trend is observed in the overall roughness of the PLLA films [Fig. 3(G)]. Increasing SNP additive content resulted in a reduction in the roughness of the surface of the PLLA films.

**TABLE I**
**Summary of all the PLLA Thin Film Coatings Synthesized and the Different Experiments Conducted on Them to Study Their Various Properties**

| Type of coatings | SEM | AFM | Antimicrobial activity | Silver release (ICP-OES) | Cytotoxicity (flow cytometry) | Cytotoxicity (FL microscope) | Tensile testing |
|---|---|---|---|---|---|---|---|
| No SNP | + | + | + | | + | + | + |
| HPC | + | | | | | | |
| 5000 ppm SNP | + | + | | | + | + | |
| 2000 ppm SNP | | | | | + | | |
| 1500 ppm SNP | | | | | + | | |
| 1000 ppm SNP | | | | | + | | |
| 700 ppm SNP | + | + | + | + | + | + | |
| 600 ppm SNP | | | + | | | | |
| 500 ppm SNP | | | + | | | | |
| 300 ppm SNP | | | + | | | | |
| 200 ppm SNP | | | + | | | | |
| 100 ppm SNP | | | + | | | | |
| 1 ppm SNP | | | + | | | | |
| 500 ppb SNP | | | + | | | | |
| 100 ppb SNP | | | + | | | | |
| 10 ppb SNP | | | + | | | | |

+ indicates the experiment conducted on a particular coating.

### Antimicrobial activity

*Escherichia coli* and *Staphylococcus aureus* were tested against composite coatings containing varying concentrations of SNP (Fig. 4). These species are the two most common associated with Healthcare Acquired Infections (HAI) and both have strains that are resistant to amoxicillin and methicillin, respectively.[48] The experimental objective was to generate a 3–5 log reduction in the number of viable bacterial colony forming unit (CFU) to conform to the FDA guidelines for antimicrobial device efficacy. At 700 ppm SNP, a 3-log reduction, 99.98%, was observed for *S. aureus* [Fig. 4(A)] and 4-log reduction for *E. coli*, 99.99% [Fig. 4(B)]. There was also a clear low SNP concentration threshold of $\sim$ 500 ppb, below which the reduction of bacteria was negligible. The bacterial reduction drops from 41.7% to 7.8% for *S. aureus* and 50% to 2.58% for *E. coli*, respectively, from 500 ppb to 100 ppb. The CFU values of the controls were $2.25 \times 10^7$ CFU/mL for *S. aureus* and $5.54 \times 10^5$ CFU/mL for *E. coli*. At 700 ppm, the CFU values decrease from $2.25 \times 10^7$ CFU/mL to $4.10 \times 10^4$ CFU/mL for *S. aureus* and from $5.54 \times 10^5$ CFU/mL to $5.60 \times 10^1$ CFU/mL for *E. coli*. These reductions in CFU values for *S. aureus* and *E. coli* were statistically significant with a *P*-value of 0.03.

The impact of the APTS linker on the antimicrobial activity of the SNP composite coating against both organisms was also evaluated. For a fixed SNP concentration of 500 ppb, two coatings were prepared; one with and the other without the APTS linker. There is no significant difference in bacteriocidal activity of the two preparations. The percentage difference is 0.08% and 2.7% for *S. aureus* and *E. coli*, respectively, [Fig. 4(C,D)]. The initial CFU values were $2.25 \times 10^7$ CFU/mL for *S. aureus* and $5.54 \times 10^5$ CFU/mL for *E. coli*. The bacterial count remains $1.20 \times 10^7$ CFU/mL for *S. aureus*, whereas it changes from $2.77 \times 10^5$ to $5.08 \times 10^5$ CFU/mL for *E. coli* on APTS and non-APTS coatings. These changes in CFU values for *S. aureus* and *E. coli* are statistically insignificant as the *P*-values, 0.24 and 0.056, respectively, are higher than either the 5% or 1% significance level.

### Silver release from nanocomposite coatings

The antimicrobial and cytotoxic activity of the coatings is related to the rate of silver ion release from the polymer. ICP-OES was used to determine the rate of release with respect to time in PBS solution as shown in Figure 5. The concentration of silver in PBS increased with respect to time with a total mean cumulative silver released during the first two days was 173.8 $\pm$ 45.7% ppb, and increasing steadily to 322.7 ppb on day 3, 393.1 $\pm$ 19.5% ppb on day 6, and eventually reaching a maximum total release of 395.5 $\pm$ 43.3% ppb SNP after 7 days.

### Cytotoxicity of nanocomposite coatings

The cytotoxicity of PLLA nanocomposite coatings to HeLa cells was determined by flow cytometry scatter and fluorescence analysis using Sytox green exclusion as a live/dead reporter. Cells analyzed 24 h after culture on the PLLA–SNP coatings showed a decrease in viability as SNP concentration increased from 700 to 5000 ppm. The forward scatter (FSC) versus side scatter (SSC) signals of control cells seen in Figure 6(C) showed a typical close packed and homogenous distribution, whereas the scatter plot of $H_2O_2$-treated (necrotic control) cells in Figure 6(B)

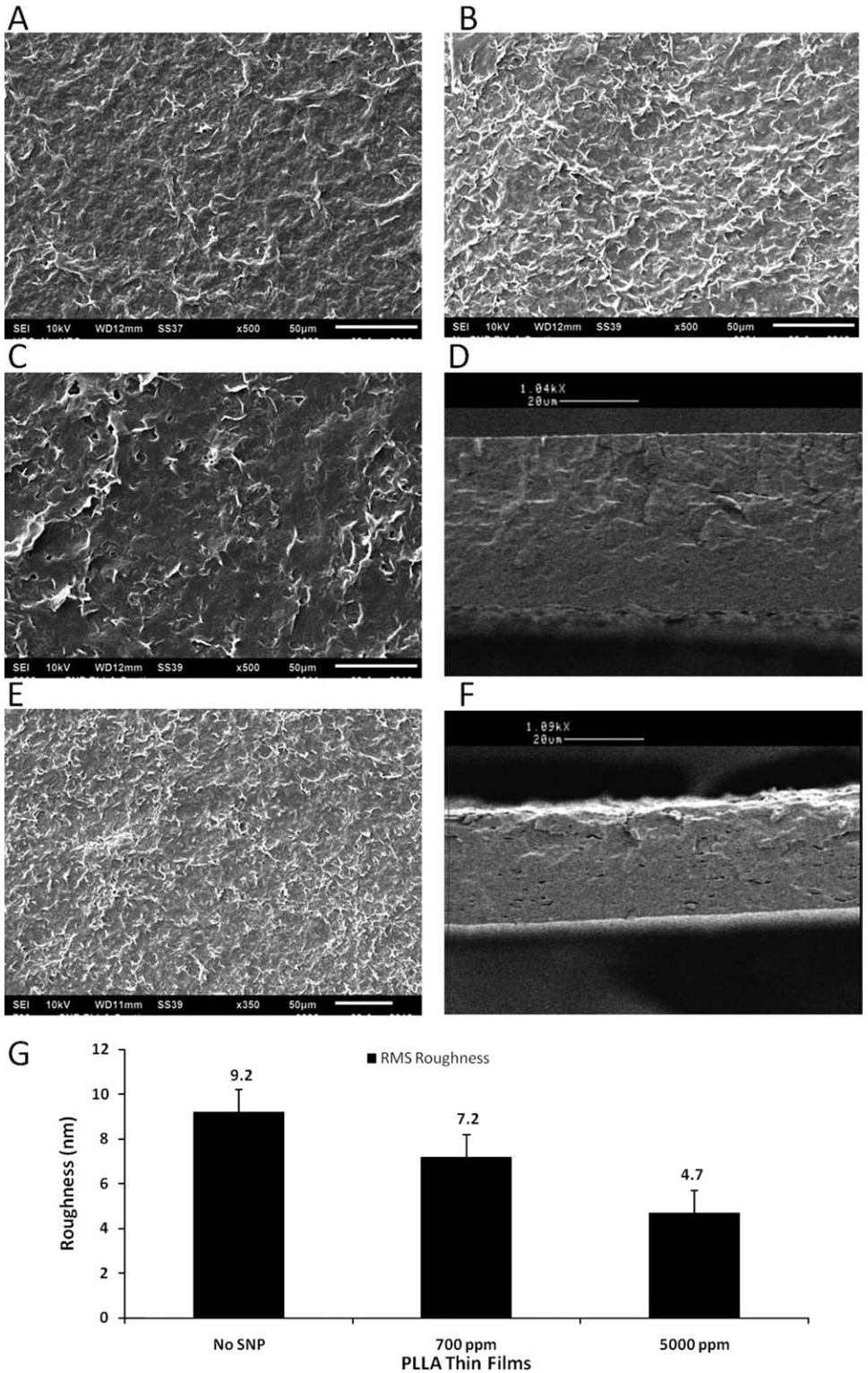


**Figure 3** SEM images of 1% PLLA thin film coatings. A: Surface of PLLA coating with No SNP and 100 µL HPC. B: Surface of PLLA coating with no SNP. C: Surface of PLLA coating with 5000 ppm SNP. D: Cross section of PLLA coating with 5000 ppm SNP. E: Surface of PLLA coating with 700 ppm SNP. F: Cross section of PLLA coating with 700 ppm SNP. G: RMS surface roughness for different PLLA–SNP films measured by AFM. The micrographs (A, B, C, and E) are ×500 magnification, whereas the cross section images (D and F) are ×1000 magnification.

showed greater SSC, correlating to the increased internal granularity and complexity in the cell debris. Cells were gated according to their scatter in region R2 for subsequent fluorescent quantification via Sytox Green fluorescence (FL1) histograms, where the marker M1 was used to calculate the

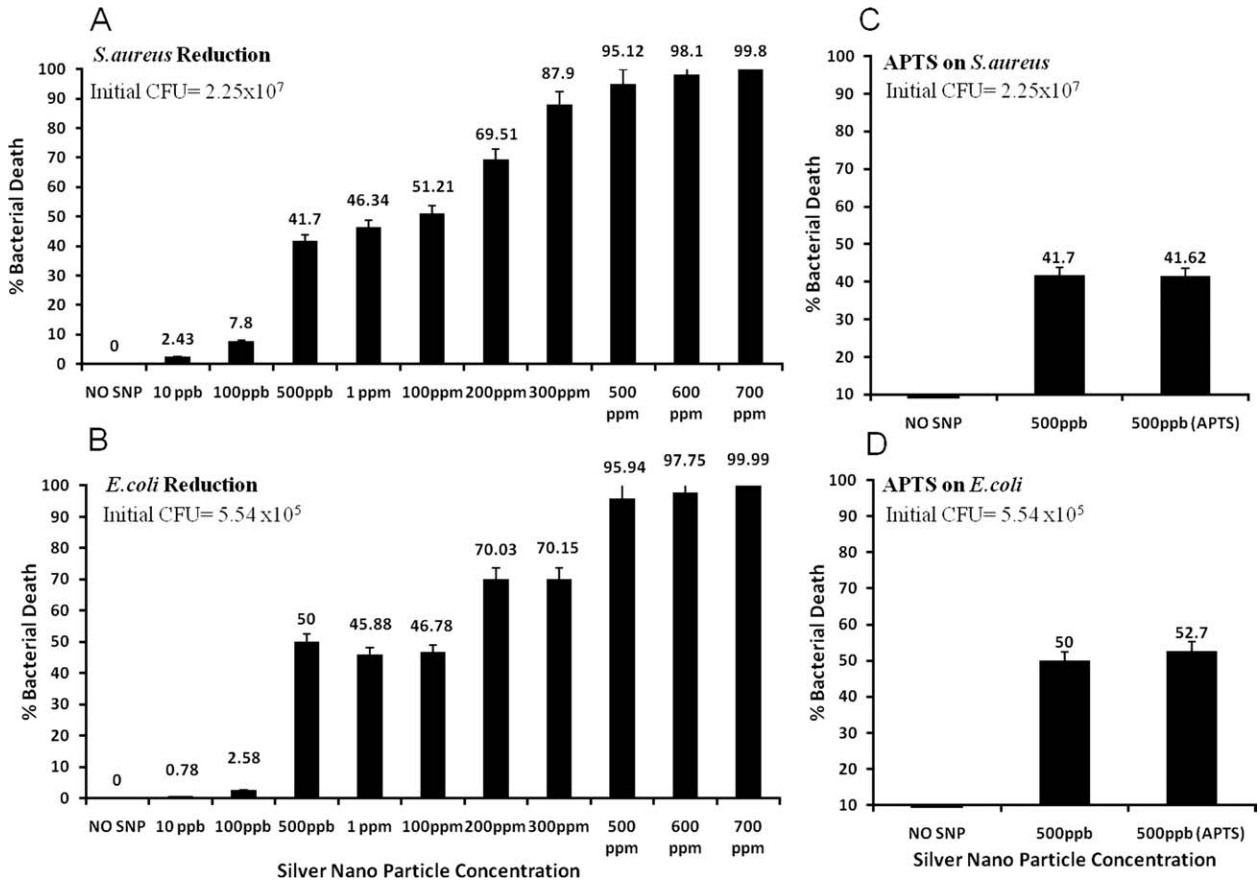


**Figure 4** Percent reduction of (A) *S. aureus* and (B) *E. coli* when exposed to varying concentrations of SNP. Reduction of (C) *S. aureus* and (D) *E. coli* with and without APTS linker, both having a fixed SNP concentration of 500 ppb ($n = 3$).

percentage of dead cells per sample [Fig. 6(B–E)]. The SNP concentration of 700 ppm, which showed effective bacteriocidal activity, had no significant difference in cell viability from live control (81.4 ± 26.9% viable for 700 ppm, Figure 6(D), versus 82.4 ± 5.11% viable for live control, Figure 6(C); $P = > 0.05$). Moderate HeLa cell toxicity was observed at SNP concentrations of 1000 ppm or greater as shown in Figure 6(A).

The analysis of bright field images in Figure 7 indicate that increasing concentrations of SNP in PLLA thin film coatings affected the morphology of the HeLa cells. The cell density and the morphology of the HeLa cells cultured on no-SNP control and 700 ppm SNP sample was very similar [Fig. 7(B,C)], whereas the cell density was reduced and cells appear rounded and stressed on 5000 ppm SNP coatings.

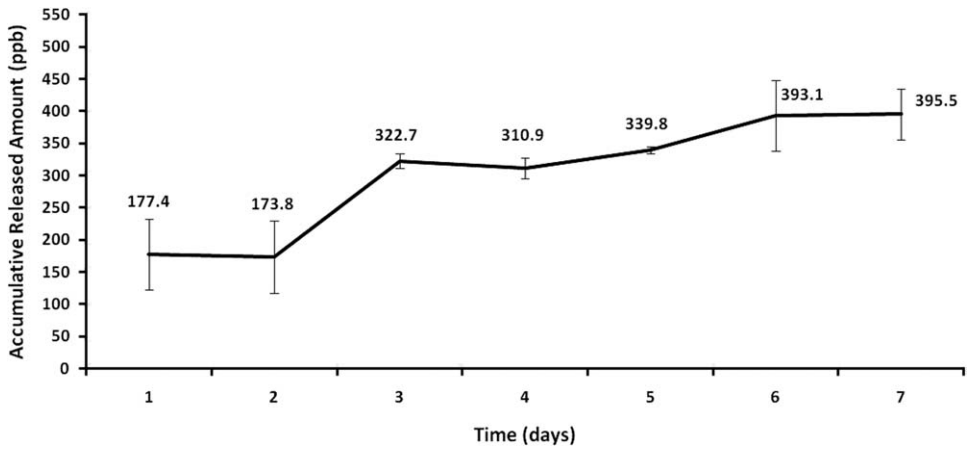


**Figure 5** Silver release from the PLLA coatings over a period of 7 days as measured by ICP-OES ($n = 2$).

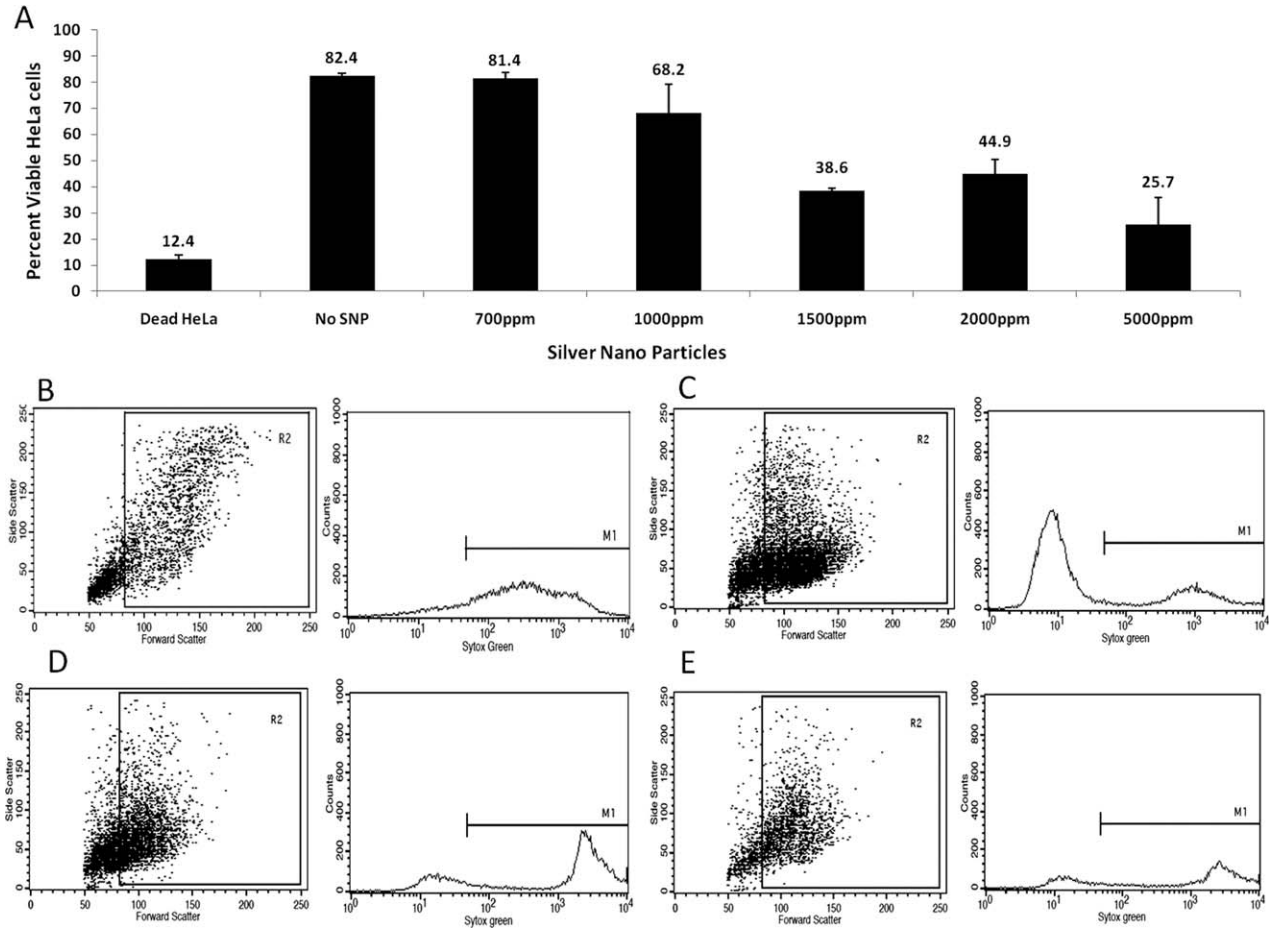


**Figure 6** Reduction of viable HeLa cultured on PLLA–SNP composites (A). Graph includes positive and negative controls. (B–E) FSC versus SSC and Sytox Green fluorescence (FL1) histograms of dead control (B), NO SNP (C), 700 ppm SNP (D), and 5000 ppm SNP (E).

### Tensile testing

The adhesion of the PLLA coatings was greatly improved by addition of a self assembling monolayer (SAM) of APTS as an interlayer between the oxide surface and PLLA coating. Non SNP control PLLA coatings cast without APTS SAM failed the standard adhesive tape test and the tensile adhesion strength for this coating was assumed as 0 MPa. For the glass control without PLLA coatings, the adhesion strength was measured to be 115.6 ± 5% MPa, the force required to delaminate the double-sided tape from the bottom glass surface of a petri dish. The tensile stress required to induce delamination of the SNP PLLA composite coatings with addition of the SAM was 282.4 ± 5% MPa [Fig. 1(B)].

## DISCUSSION

These results demonstrate that SNP can produce in a facile, room temperature, one pot synthesis using HPC biomass as a templating/stabilizing agent. These particles are soluble in a variety of polar organic solvents allowing practical incorporation into a biocompatible composite coating to provide antimicrobial functionality. The novel biomass-mediated chemical reduction and purification method described in this work yields a high purity, concentrated particle that is readily dispersed in the PLLA polymer resin. Using this method, 700 ppm concentration of SNP in PLLA can be achieved with little impact on mechanical stability and adhesion strength.

The ISO 22196 antimicrobial test standard, with minimal modifications, was chosen for the challenge assays to increase the regulatory relevance of the testing and allow convenient comparisons to previously published results. A 24 h exposure period was selected to represent the critical perioperative time frame for surgical site infection. The 3- and 4-log reductions of representative gram-positive and -negative bacteria fall within the realm of clinically relevant performance previously demonstrated for antibiotic-based PLLA composite orthopedic coatings.[49] The results indicate that *S. aureus* is more resistant to silver inactivation than *E. coli*. This may be related to the thick peptidoglycan layer of gram-positive bacteria.

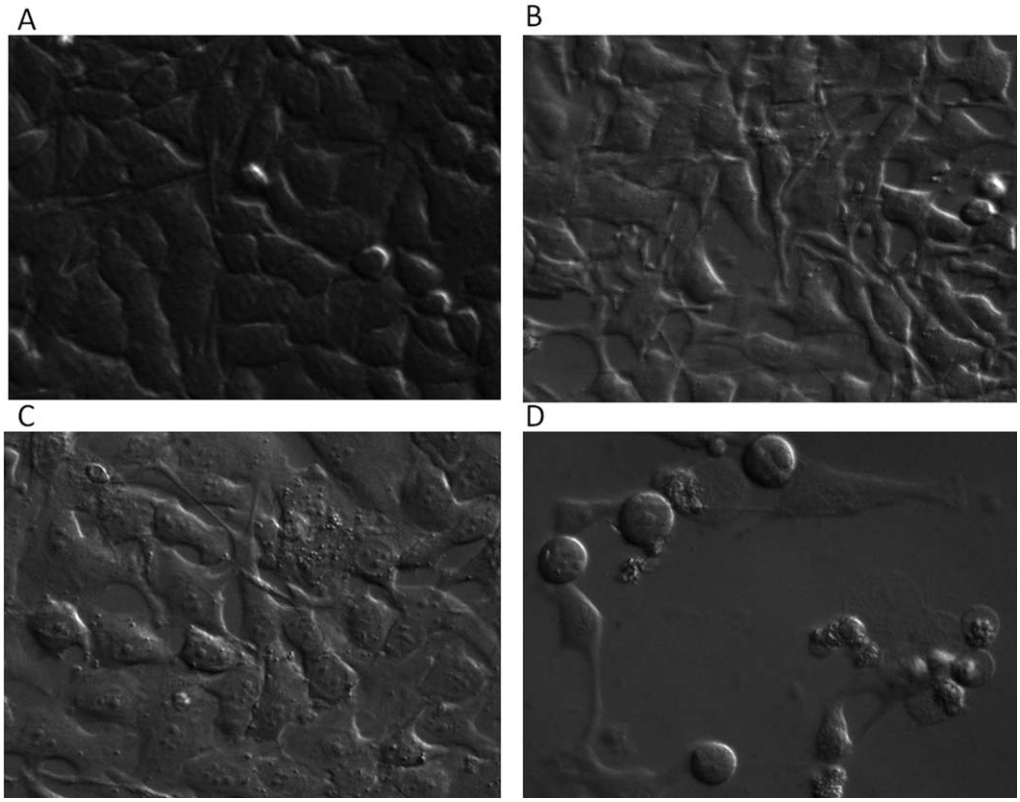


**Figure 7** A: The morphology of live HeLa cells on the surface of 12-well tissue cultured plate. Bright field images showing the viability of HeLa cells when grown on the surface of PLLA thin films containing (B) No SNP, (C) 700 ppm, and (D) 5000 ppm of SNP. The cells with compromised membranes (dead cells) detach from the surface of PLLA films at 5000 ppm of SNP. All images are ×400 magnifications.

To date, SNP containing biocompatible nanocomposites have not had practical clinical value due to the lack of high purity nanoparticle systems which are compatible with biopolymer processing conditions. The current system addresses this challenge with the addition of hydroxypropyl cellulose (HPC), a hydrophilic polymer derived from biomass with hydroxyl groups acting to template,[50] stabilize the particle, and provide a convenient mechanism for concentration and purification. HPC is a thermoresponsive compound and flocculates at elevated temperatures which facilitate synthesizing concentrated, highly pure, and polymer-compatible SNPs. The thermally mediated flocculation and concentration step allowed the bulk of the residual reaction by products to be removed by serial flocculation, washing, and resuspension. Additionally, the biomass acts to improve nanoparticle solubility in polar solvents. Concentrations of SNP up to 0.5%/wt of PLLA could be maintained as colloidal dispersion during processing.

Solvents for casting were carefully chosen to reduce potential cytotoxic and antibacterial side effects. Also, the solvent had to be miscible with the polar solvents used to dissolve powdered SNP. Methanol was used as a solvent for dispensing HPC-stabilized SNP complexes in PLLA containing solution. Methanol was easily removed from the cast polymer by heating and washing with DI water. Controlled drying conditions were critical to the formation of reproducible thin films. Drying at 25°C with negligible air flow aided in the formation of low stress polymer and homogenous coatings.

Increasing SNP content resulted in a reduction of surface roughness as demonstrated by SEM and AFM. Results from control, HPC containing, PLLA coatings suggest the correlation is related to HPC content and not the SNP.

The antimicrobial efficacy of these coatings is based on the efficiency of silver release from the polymer. Determining the rate of silver release with respect to time and correlating these results with bacteriocidal performance allows the generation of design heuristics for the composite coatings. The release at 24 h, 177.4 ppb, resulted in a reduction of 99.99% and 99.8% of *E. coli* and *S. aureus*, respectively, while remaining noncytotoxic to HeLa cells. The total silver released during the 7 days experiment was $\sim$ 2.25 greater by the rate of release declined rapidly after the initial bolus. Given the low concentration of silver in solution this is attributed to a reduction in accessible SNP as opposed to saturation of the solution.

The adhesion of the nanocomposite coating is critical for use indwelling applications as cracking and delamination could result in inflammation, immune response, and/or tissue damage. Stress as a result of differences in thermal expansion coefficients of the film and the glass petri dishes could be managed by the addition of a silane-based self assembling monolayer SAM, APTS. After surface polymerization, the amino-terminated side chain is presented normal to the surface allowing for interaction with the PLLA composite. By casting and bonding the films on the glass surface, the extrinsic stress was eliminated, as both materials are constrained in the lateral directions and the stresses develop equally. The adhesion of the PLLA coatings in this study was greatly improved by the addition of APTES as the force required to induce delamination of the final engineered SNP PLLA composite coatings was measured as 282.4 ± 5% MPa [Fig. 1(A)] without negatively affecting the antimicrobial performance. Based upon the force required to delaminate the PLLA thin film, it is believed that the silane–PLLA interaction at the interface is an ionic-dipole chemical interaction.[51]

A flow cytometry viability assay, conducted using HeLa cells stained using Sytox Green to indicate cell necrosis, demonstrated that there is a substantial difference in mammalian and bacterial cell responses to SNP. The SNP concentrations of 700 ppm caused a 1000-fold decrease in viable bacteria, but had no effect on HeLa cell viability. Qualitative observations made by bright-field microscope support these conclusions as no changes in HeLa cell density or morphology were observed in control coatings or those with 700 ppm SNP, whereas density and morphology of cells grown on coatings containing 5000 ppm were substantially different. While these data suggest a viable antimicrobial construct, further testing is necessary to determine *in vitro* and *in vivo* toxicity of SNP–PLLA nanocomposites across diverse cell and tissue types for extended durations.

## CONCLUSIONS

In this study, the formation of SNP–PLLA nanocomposites compatible with indwelling device environments was demonstrated by using a novel biomass-mediated synthesis method. The resulting 25–75 nm SNP are biocompatible, nonagglomerated, high purity, and soluble in a variety of polar solvents. The biocompatible/bioabsorbable PLLA nanocomposites synthesized with the biomass-stabilized particles reduce viable *S. aureus* and *E. coli* bacterial CFU's by 99.98–99.99%, respectively. This strategy for particle synthesis and coating formation shows promise for potential application in reducing perioperative surgical site infections associated with chronic indwelling devices.

Further evaluation of the antimicrobial and cytotoxic behavior of PLLA nanocomposite coatings on simulated implantable device surfaces will be required to determine the impact of substrate composition on the physio–chemical properties of the coatings. Mechanical properties such as hardness, resistance to frictional wear, and debris generation will be critical to the clinical performance of nanocomposite coatings. Additionally, future experiments conducted both *in vivo* and *in vitro* will explore the biocompatability of the nanocomposites such as biodegradation rates, degradation products, thrombogenesis, and induction of inflammatory response.

The authors are thankful to Ms. Marilyn Dietrich, Pathobiological Science Department-LSU, for flow cytometer analysis, Ms. Cindy Henk and Ms. Ying Xiao, Biological Science Department-LSU, for SEM analysis, Dr Robert Gambrell, Wetland Biogeochemistry Department, for the ICP-OES analysis. This manuscript was approved for publication by the director of the Louisiana Agricultural Experiment Station as number 2010-232-5243.

## References

1. Ozcan, S. K. Turk Klin Tip Bilim Derg 2007, 27, 589.
2. Rodriguez-Martinez, J. M.; Pascual, A. Rev Med Microbiol 2006, 17, 65.
3. Tamilvanan, S.; Venkateshan, N.; Ludwig, A. J Control Release 2008, 128, 2.
4. Kwakye-Awuah, B.; Williams, C.; Kenward, M. A.; Radecka, I. J Appl Microbiol 2008, 104, 1516.
5. Abedi, D.; Mortazavi, S. M.; Mehrizi, M. K.; Feiz, M. Text Res J 2008, 78, 311.
6. Roe, D.; Karandikar, B.; Bonn-Savage, N.; Gibbins, B.; Roullet, J. B. J Antimicrob Chemother 2008, 61, 869.
7. Damm, C.; Munstedt, H. Appl Phys A Mater Sci Process 2008, 91, 479.
8. Burkatovskaya, M.; Castano, A. P.; Demidova-Rice, T. N.; Tegos, G. P.; Hamblin, M. R. Wound Repair Regen 2008, 16, 425.
9. Raad, I.; Reitzel, R.; Jiang, Y.; Chemaly, R. F.; Dvorak, T.; Hachem, R. J Antimicrob Chemother 2008, 62, 746.
10. Percival, S. L.; Bowler, P.; Woods, E. J. Wound Repair Regen 2008, 16, 52.
11. Lorente, L.; Lecuona, M.; Ramos, M. J.; Jimenez, A.; Mora, M. L.; Sierra, A. Infect Control Hosp Epidemiol 2008, 29, 1171.
12. Adair, C. G.; Gorman, S. P.; Feron, B. M.; Byers, L. M.; Jones, D. S.; Goldsmith, C. E.; Moore, J. E.; Kerr, J. R.; Curran, M. D.; Hogg, G.; Webb, C. H.; McCarthy, G. J.; Milligan, K. R. Intensive Care Med 1999, 25, 1072.
13. Jones, D. S.; McGovern, J. G.; Woolfson, A. D.; Adair, C. G.; Gorman, S. P. Pharm Res 2002, 19, 818.
14. Olson, M. E.; Harmon, B. G.; Kollef, M. H. Chest 2002, 121, 863.
15. Johnson, J. R.; Kuskowski, M. A.; Wilt, T. J. Ann Intern Med 2006, 144, 116.
16. Elliott, T. S. J. J Hosp Infect 2007, 65, 34.
17. Loertzer, H.; Soukup, J.; Hamza, A.; Wicht, A.; Rettkowski, O.; Koch, E.; Fornara, P. Transplant Proc 2006, 38, 707.
18. Lansdown, A. J Wound Care 2002, 11, 125.
19. Sondi, I.; Salopek-Sondi, B. J Colloid Interface Sci 2004, 275, 177.
20. Stobie, N.; Duffy, B.; McCormack, D. E.; Colreavy, J.; Hidalgo, M.; McHale, P.; Hinder, S. J. Biomaterials 2008, 29, 963.
21. Sambhy, V.; MacBride, M. M.; Peterson, B. R.; Sen, A. J Am Chem Soc 2006, 128, 9798.

22. Darouiche, R.; Raad, I.; Heard, S.; Thornby, J.; Wenker, O.; Gabrielli, A.; Berg, J.; Khardori, N.; Hanna, H.; Hachem, R. N Engl J Med 1999, 340, 1.
23. Greenfeld, J.; Sampath, L.; Popilskis, S.; Brunnert, S.; Stylianos, S.; Modak, S. Crit Care Med 1995, 23, 894.
24. Tan, S.; Ouyang, Y.; Zhang, L.; Chen, Y.; Liu, Y. Mater Lett 2008, 62, 2122.
25. Khare, M. D.; Bukhari, S. S.; Swann, A.; Spiers, P.; McLaren, I.; Myers, J. J Infect 2007, 54, 146.
26. Cowan, M. M.; Abshire, K. Z.; Houk, S. L.; Evans, S. M. J Ind Microbiol Biotechnol 2003, 30, 102.
27. Dritch, E.; Marino, A.; Malakanok, V.; Albright, J. J Trauma Injury Infect Crit Care 1987, 27, 301.
28. Koh, J. H.; Seo, J. A.; Park, J. T.; Kim, J. H. J Colloid Interface Sci 2009, 338, 486.
29. Shirokova, L. N.; Alexandrova, V. A.; Egorova, E. M.; Vihoreva, G. A. Appl Biochem Microbiol 2009, 45, 380.
30. Shanmugam, S.; Viswanathan, B.; Varadarajan, T. K. Mater Chem Phys 2006, 95, 51.
31. Guillemot, G.; Despax, B.; Raynaud, P.; Zanna, S.; Marcus, P.; Schmitz, P.; Mercier-Bonin, M. Plasma Process Polym 2008, 5, 228.
32. Mukherjee, P.; Ahmad, A.; Mandal, D.; Senapati, S.; Sainkar, S. R.; Khan, M. I.; Parishcha, R.; Ajaykumar, P. V.; Alam, M.; Kumar, R.; Sastry, M. Nano Lett 2001, 1, 515.
33. Dickson, D. P. E. J Magnetism Mag Mater 1999, 203, 46.
34. Mann, S. Nature 1993, 365, 499.
35. Oliver, S.; Kuperman, A.; Coombs, N.; Lough, A.; Ozin, G. A. Nature 1995, 378, 47.
36. Pum, D.; Sleytr, U. B. Trends Biotechnol 1999, 17, 8.
37. Sleytr, U. B.; Messner, P.; Pum, D.; Sara, M. Angew Chem Int Ed 1999, 38, 1035.
38. Mandal, D.; Bolander, M. E.; Mukhopadhyay, D.; Sarkar, G.; Mukherjee, P. Appl Microbiol Biotechnol 2006, 69, 485.
39. Klaus, T.; Joerger, R.; Olsson, E.; Granqvist, C. G. Proc Natl Acad Sci USA 1999, 96, 13611.
40. Haefeli, C.; Franklin, C.; Hardy, K. J Bacteriol 1984, 158, 389.
41. Kramer, R. M.; Li, C.; Carter, D. C.; Stone, M. O.; Naik, R. R. J Am Chem Soc 2004, 126, 13282.
42. Chandra, R.; Taneja, P.; John, J.; Ayyub, P.; Dey, G. K.; Kulshreshtha, S. K. Nanostruct Mater 1999, 11, 1171.
43. Karthikeyan, J.; Berndt, C. C.; Tikkanen, J.; Reddy, S.; Herman, H. Mater Sci Eng A Struct Mater Prop Microstruct Process 1997, 238, 275.
44. Greil, J.; Spies, T.; Böswald, M.; Bechert, T.; Lugauer, S.; Regenfus, A.; Guggenbichler, J. Infection 1999, 27, S34.
45. Thirumala, S.; Forman, J. M.; Monroe, W. T.; Devireddy, R. V. Nanotechnology 2007, 18, 12.
46. Patakfalvi, R.; Oszko, A.; Dekany, I. Colloid Surf A Physicochem Eng Asp 2003, 220, 45.
47. Shukla, S.; Seal, S.; Mishra, S. R. J Sol-Gel Sci Technol 2002, 23, 151.
48. Moumile, K.; Carbonne, A.; Rouquet, M. L.; Gamard, M. N.; Bornand-Rousselot, A.; Jarlier, V.; Cambau, E. Pathol Biol 2004, 52, 557.
49. Kalicke, T.; Schierholz, J.; Schlegel, U.; Frangen, T. M.; Ĥller, M.; Printzen, G.; Seybold, D.; Ĥlckner, S.; Muhr, G.; Arens, S. J Orthop Res 2006, 24, 1622.
50. Clasen, C.; Kulicke, W. M. Prog Polym Sci 2001, 26, 1839.
51. Awaja, F.; Gilbert, M.; Kelly, G.; Fox, B.; Pigram, P. J. Prog Polym Sci 2009, 34, 948.